

# Direct Measurement of Energy Loss Due to Aging Effects in the Condensed Phase Explosive PBX 9404

Scott I. Jackson\*, Eric K. Anderson, and Larry G. Hill

*Explosive Science and Shock Physics Division, Los Alamos National Laboratory, Los Alamos, NM 87507 USA*

---

## Abstract

The explosive performance of PBX 9404, a condensed phase explosive with HMX and nitrocellulose reactive ingredients, was evaluated using the detonation cylinder expansion test after it had been naturally aged for over 46 years. Nitrocellulose is known to chemically degrade with age, but the corresponding effect on explosive performance is currently unknown. Two new cylinder tests were fielded with the oldest known PBX 9404 explosive (>46 years) and the data was compared with prior PBX 9404 cylinder test data. A method for comparing wall motion data collected by streak camera and laser interferometry diagnostics was also introduced. Analysis of the cylinder motion indicated that the aged explosive exhibits decreased performance, which varied with cylinder expansion radius and product specific volume. This energy decrement was found to be 0.8% of the total initial explosive energy per decade of age at a product volume of 7.0 cc/g. The measured energy decrement in explosives older than 37 years exceeds the chemical energy content of nitrocellulose, indicating that nitrocellulose decomposition radicals are likely degrading the normally stable HMX molecules during the aging process.

### Keywords:

Detonation, Cylinder Test, Equation of State

---

## 1. Introduction

The extreme product conditions developed by detonation of condensed phase explosives provides the means to perform high rates of work on adjacent materials [1]. For engineering applications, it is desirable to predict the possibility of any explosive performance variation due to varying storage conditions or duration. One possible source of variation is decreased chemical energy content of the explosive from aging [2–5]. Explosives usually consist of mixtures of organic molecules with large chemical potential energy. These metastable compounds can be modified by thermal and photochemical processes to partially decompose, developing less chemical potential energy and altered mechanical properties. Prediction of these effects remains difficult due to the unknown kinetics associated with these low-rate decomposition reactions as well as difficulties in determining what, if any, chemical modifications have occurred in formulated explosive charges [6–12].

There have been very few direct measurements of this effect as formulations are typically selected to be relatively stable over long times (decades). Thus, quantifying any performance changes requires very long study timescales and high measurement precision. Artificial aging studies, which store explosives at elevated temperatures, are often conducted to address these issues, but can yield unrealistic results due to the strongly non-linear temperature dependence of chemical kinetics.

The explosive PBX 9404 has been a subject of considerable aging studies [2, 4, 6–12]. Composed of 94 wt% HMX, 3 wt% tris- $\beta$  chloroethylphosphate (CEF) plasticizer, 2.9 wt% nitrocellulose (NC), and 0.1 wt% diphenylamine (DPA) as a stabilizing agent [13], PBX 9404 is known to exhibit variations with age, presumably as the NC decomposes. The explosive has been observed to change color from white when new, to light blue, dark blue, and finally yellow-brown as the nitrogen-based decomposition products accumulate [11, 13].

Most prior work over the past fifty years has assumed that age-based performance degradation in PBX 9404 is solely due to decomposition of the NC, which is the

---

\*Corresponding author:

Email address: [sjackson@lanl.gov](mailto:sjackson@lanl.gov) (Scott I. Jackson)

least stable ingredient. Nitrocellulose decomposes autocatalytically, generating nitric acid [11] and nitrogen oxides [2], which further accelerate the NC decomposition. The DPA additive was intended to scavenge these nitrogen radicals [2, 4, 8]. However, uncertainties in the rate of NC decomposition and its stabilization capacity have led to a multi-decade effort intended to better understand this aging process [6–12]. These prior analytical chemistry studies support concerns that NC decay does indeed occur in PBX 9404, but have been insufficient to establish predictive models for the effect of aging on the explosive ingredients, the detonation kinetic details, or the resulting detonation performance.

Instead, applied measurements of the detonation product energy delivery to a metal confiner are used to provide insight into the underlying chemical kinetic variations that cannot be resolved with current technology. This approach is entirely analogous to popular gas-phase shock-tube ignition and flame-speed measurements, which use similarly applied observables (like ignition time delays or flame speeds) to develop insight into the underlying chemical kinetics. To date, the only prior published record on this topic is by Hill et al. [12], who verified performance degradation with age but was not able to provide quantitative estimates or uncertainties due to a limited amount of experimental data.

In this work, we directly measure the performance degradation in naturally aged PBX 9404 explosive with cylinder expansion (CYLEX) experiments, which characterize the explosive energy of PBX 9404 samples over a period of at least 46 years, the longest aging duration ever characterized for this material. Our analysis corrects for differences in diagnostic methods used over this period. PBX 9404 is shown to lose energy output with age at a rate of approximately 0.8% of its total initial chemical energy content per decade, corresponding to 3.7% of its initial chemical energy content over a 46 year period.

These results indicate that the energy loss actually exceeds the energy content of the pristine NC, implying that both NC *and* HMX molecules must be also be altered by the NC decomposition radicals. While not widely considered previously due to its increased complexity, this concept is supported by limited prior measurement and theory: The NC in PBX 9404 has been observed to degrade faster than neat NC [14]; HMX-NC blends are known to create unique bonds [15]; and the NC decomposition radicals generated are highly reactive and able to modify otherwise stable nearby molecules. Our results thus indicate that the normally stable explosive molecules can be degraded by less stable chemical ingredients present in explosive formula-

tions and that future PBX 9404 aging studies should analyze blends of HMX and NC, rather than each ingredient individually.

## 2. Cylinder Expansion Test Data on PBX 9404

The CYLEX test is a standard performance experiment used to quantify the product energy of a condensed-phase explosive [16–19]. The test configuration consists of an inert and ductile confiner tube tightly encasing an explosive rod. Detonation initiated at one

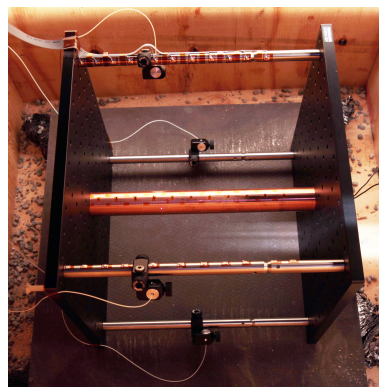


Figure 1: The cylinder test assembly. Shorting wire stations can be seen taped to the top of the tube in each image. The illumination location of one of the PDV probes (bottom left side of tube) is shown with red laser light.

end travels along the rod length. High-pressure products accelerate the confiner outwards [19] and the motion history is recorded with a diagnostic. The confiner rapidly accelerates at first, typically in a compressible fashion, and then approaches a terminal velocity at later times, in an incompressible motion regime [20]. This motion is used to evaluate the explosive performance and product equation of state [1, 16–19].

PBX 9404 has been in existence for six decades and its performance was previously characterized. In the current study, three main sources of prior data have been identified for comparison. We also present data from two recent CYLEX tests using the oldest PBX 9404 tested to date. All data and sources are summarized in Table 1 and described below. All explosives were stored in unheated indoor earth-covered storage magazines, with no humidity control, where the temperature varied seasonally between 4–20° C in a low-humidity desert environment. These temperature and humidity variations are quite limited when compared to artificial aging studies, which control the explosive temperature and humidity for a very short period of time at unrealistically harsh conditions.

Table 1: PBX 9404 standard-scale CYLEX data. Initial explosive density, detonation velocity, inner diameter, and outer diameter are  $\rho_0$ ,  $D_0$ , ID, and OD respectively. The superscript (\*) indicates that the explosive was aged as molding powder and not as a pressed charge.

Lab	Identifier	$\rho_0$ (g/cc)	$D_0$ (mm/ $\mu$ s)	ID (mm)	OD (mm)	Streak or PDV	Age (Years)	Ref.
LLNL	K260235	1.845	$8.782 \pm 0.009$	25.430	30.617	Streak	<3	McMurphy [21]
LLNL	K260237	1.845	8.665	25.427	30.618	Streak	<3	McMurphy [21]
LLNL	K260273	1.843	$8.783 \pm 0.059$	25.433	30.648	Streak	<3	McMurphy [21]
LANL	C4526	1.847	$8.787 \pm 0.001$	25.43	30.62	Streak	3.5	Campbell and Engelke [22]
LANL	C4527	1.847	$8.783 \pm 0.001$	25.43	30.62	Streak	3.5	Campbell and Engelke [22]
LANL	8-1292	1.845	$8.791 \pm 0.005$	25.41	30.50	PDV	37.5*	Hill et al. [23]
LANL	8-1293	1.845	$8.787 \pm 0.003$	25.41	30.48	Both	37.5*	Hill et al. [23]
LANL	8-1874	1.845	$8.810 \pm 0.005$	25.41	30.48	PDV	>46	this work
LANL	8-1875	1.845	$8.802 \pm 0.004$	25.41	30.48	PDV	>46	this work

### 2.1. Prior Tests with Streak Diagnostic

CYLEX data fielded with streak diagnostics is available for PBX 9404 from three sources. McMurphy [21] reports three standard scale tests with full data return. These tests have identifiers K260235, K260237, and K260273. Tests K260235 and K260237 were fielded in 1967, while K260273 was fielded in 1973. The explosive age was unknown, but assumed to be <3 years before test execution due to the fact that PBX 9404 was being actively formulated during the test period. Wall motion was characterized with a streak camera and archived as wall radius versus time profiles consisting of approximately 50 data points per test, as shown in Fig. 2 (Top). McMurphy [21] also differentiated these data in time to yield the rate of increase in the wall radius with time at the axial location of the streak camera slit (Fig. 2 Bottom). This value, which we refer to as the radial increase rate, is *not* the true wall velocity, but rather an artificially high phase velocity resulting from the interaction of the angled cylinder wall with the streak measurement line as discussed in Jackson [19].

Campbell and Engelke [22] report streak camera records from two PBX 9404 cylinder tests, C4526 and C4527, fielded at LANL (Los Alamos National Laboratory) in 1975. Their tests used 3.5 year old explosive (produced in December 1971) at the time of testing, from the last PBX 9404 lot ever formulated, lot HOL620-5 with LANL designation #43 or 5-620(43). Hill et al. [23] reprocessed the streak film of Campbell and Engelke [22] at high resolution (Fig. 2 Top). Fig. 2 (Bottom) plots velocity-time histories as computed by Campbell and Engelke [22] via differentiation of a 7th-order polynomial fit to their position-time data.

The position-time traces of Fig. 2 are consistent to within  $\pm 1\%$ . The velocity-time traces have higher deviations associated with discrete differentiation errors. During the compressible motion phase, deviations of up to 30% in velocity exist between tests. In the late-

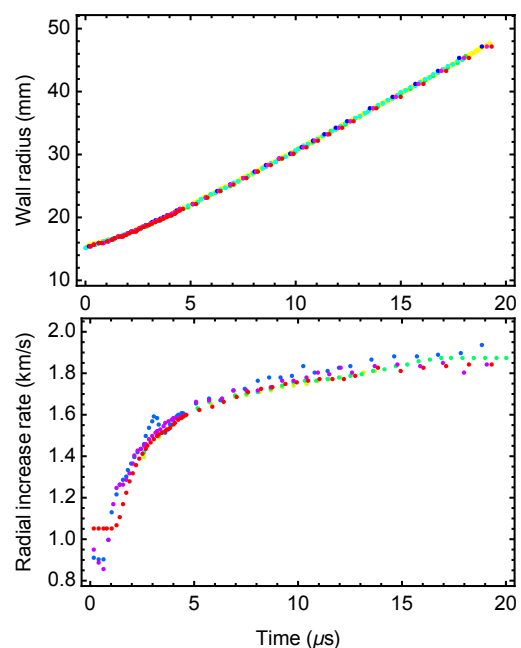


Figure 2: Wall radius versus time profiles from cylinder tests: 8-1293 (yellow) [23], C4526 (green) [22], C4527 (cyan) [22], K260235 (blue) [21], K260237 (magenta) [21], and K260273 (red) [21].

time incompressible motion phase, test-to-test variation is approximately 5% in velocity. The data of Campbell and Engelke [22] is more consistent, possibly as both tests were fielded by the same researchers, with deviations not exceeding 0.5% in position-time, 10% in velocity for the compressible regime, and 4% in velocity for the incompressible regime. Despite this, the streak diagnostic is not able to adequately resolve the ringing wall motion in the compressible regime (Fig. 2 Bottom).

### 2.2. Prior Tests with Streak and PDV Diagnostics

Hill et al. [23] fired two cylinder tests with PBX 9404, identified as 8-1292 and 8-1293, at LANL. Their tests utilized the same explosive lot as Campbell and

Engelke [22], which was 37.5 years old when fielded in 2009. Unlike all other experiments in this work, the explosive from Hill et al. [23] was stored as unpressed molding powder. It was only pressed to shape just prior to machining and testing in 2009, thus any NC mass loss due to binder degradation prior to pressing would have resulted in a higher energy density explosive due to the higher-than-normal ratio of HMX to binder. The cylinders of Hill et al. [23] and those fielded for the present study had slightly thinner walls than in historic experiments (Table 1).

Hill et al. [23] used both PDV and streak camera diagnostics simultaneously to record the wall motion on 8-1293, with PDV probes tilted  $7^\circ$  off-normal upstream for improved signal return. Only PDV data is available for 8-1292. The PDV traces, shown in Fig. 3 (Top), exhibit excellent agreement across tests with deviations of 4% in the compressible regime and less than 2% in the incompressible regime. Streak data from 8-1293 is shown in Fig. 4 and used below to relate the PDV and streak measurements.

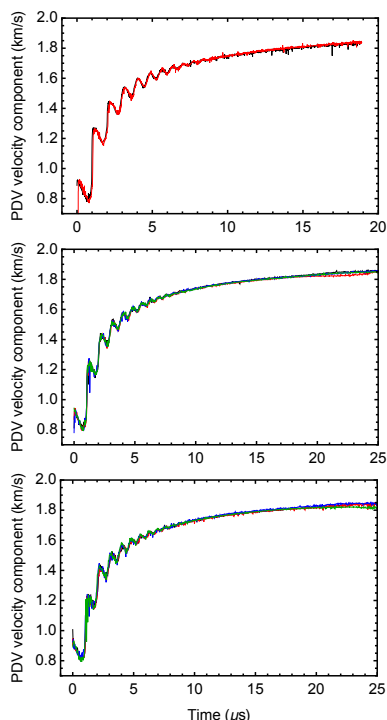


Figure 3: Cylinder wall velocity component as measured by PDV probes for: Top: Tests 8-1292 (black) and the 8-1293 (red) with probes  $7^\circ$  off normal and tilted towards the detonator; Middle: Test 8-1874 with PDV1 (Black), PDV2 (Red), PDV3 (Blue), and PDV4 (Green); Bottom: 8-1875 with PDV1 (Black), PDV2 (Red), PDV3 (Blue), and PDV4 (Green). The timebase of each probe has been shifted such that first motion corresponds to the time origin.

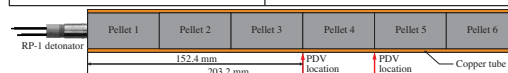
### 2.3. Recent Experiments with PDV Diagnostics

Two CYLEX experiments, 8-1874 and 8-1875, were fielded in 2015 with PBX 9404 to provide additional data for analysis. Test assemblies were consistent with earlier methods, consisting of a copper tube supported by an aluminum and steel structure as shown in Fig. 1. Cylinder diameters are shown in Table 1. The total tube length was 304.8 mm and its density was 8.984 g/cc. The tube was oxygen-free high thermal conductivity (OFHC) C101 copper with a dead soft temper. Metallurgical analysis verified it was in an annealed state after machining (8-20 Rockwell F hardness) with grain sizes on the order of  $50 \mu\text{m}$ .

Each cylinder was filled with PBX 9404 explosive that had been machined into multiple pellets to achieve good dimensional tolerances. Each pellet was  $25.4 \pm 0.025$  mm in OD and  $50.8 \pm 0.025$  mm in length. Pellets from 8-1874 and 8-1875 were machined from billets labelled 10114Y4608-02 and 10114Y4601-02, respectively. The complete history of the billets is not known, but they were both received by Sandia National Laboratory as hydrostatically pressed billets in 1969, making them over 46 years old at the date of testing. Immersion density measurements of numerous billets (including the ones selected for testing) of similar age did not exhibit anomalously low densities, indicating that naturally aged PBX 9404 does not exhibit mass loss and any decomposition radicals are likely retained in the material. Pellets were arranged in order of increasing density in the direction of detonation propagation (Table 2). Due to machining tolerances, annular voids on the or-

Table 2: PBX 9404 pellet densities and locations.

Test	Pellet	Density (g/cc)	Test	Pellet	Density (g/cc)
8-1874	1	1.8454	8-1875	1	1.8463
8-1874	2	1.8455	8-1875	2	1.8463
8-1874	3	1.8456	8-1875	3	1.8463
8-1874	4	1.8457	8-1875	4	1.8463
8-1874	5	1.8457	8-1875	5	1.8463
8-1874	6	1.8457	8-1875	6	1.8463



der of  $10 \mu\text{m}$  or smaller were likely present between the copper and explosive and were filled with Dow Corning Sylgard 184 Silicone Elastomer to prevent product jetting ahead of the detonation. Each test was initiated with a Teledyne RISI RP-1 detonator glued to the center of the first pellet.

The propagation of the detonation front along the length of each cylinder was measured using 11 equally spaced shorting wires in similar fashion to that of Jack-

son [20]. Detonation velocities were determined from a linear fit to the shorting probe data, were approximately 40 m/s faster than previous tests, and showed low standard errors to the linear fitting form. Examination of the  $D_0$  trend in Table 1 shows a slight increase with explosive age.

Four PDV probes were used to record the wall motion at two different axial locations located 152.4 mm (PDV1 and PDV2) and 203.2 mm (PDV3 and PDV4) downstream of the detonator. All probes were oriented normal to the initial cylinder wall position and each pair was azimuthally separated by  $90^\circ$ . Probes were located to within  $60 \mu\text{m}$  and sampled at 20 GHz (50 GS/s sample rate) during each test. The PDV data were analyzed to yield the wall velocity via a temporally sliding Fast Fourier Transform using a 1024-bit (20.5 ns) window and a 128-bit (2.6 ns) step size. The resulting PDV profiles are shown in Figs. 3 (Middle) and 3 (Bottom) for tests 8-1874 and 8-1875, respectively.

Individual traces in Figs. 3 (Middle) and 3 (Bottom) indicate excellent agreement across all probes and both tests. The velocity histories do not diverge at all until  $20 \mu\text{s}$ , which is late in the test sequence when the cylinder wall begins to fail and the product pressure is low (less than 1 GPa). Agreement across the two tests is within 4% in the ringing regime and better than 2% at late times. The velocity-time features present in compressible cylinder wall motion are discussed in detail for similar tests in prior work [20].

### 3. Analysis

In this section, the CYLEX data is analyzed to quantify the effect of explosive aging on energy delivery to an adjacent metal confiner. First, we correct each dataset for the diagnostic used. We then compute the variation in the explosive energy delivery with age.

#### 3.1. Comparing Streak and PDV Data

Streak cameras image the cylinder radius at a specific axial location on the tube through a thin slit. As the cylinder expands, its radius increases with time along that radially oriented slit. However, the cylinder wall trajectory is not perfectly normal to the initial wall location, as shown in [19]. Instead, the wall tilts slightly downstream due to the finite detonation velocity. For PBX explosives, the cylinder wall angle asymptotes to approximately  $12^\circ$ . Due to this effect, the expanding cylinder also translates axially across the streak slit. Thus, the streak-camera position-time record integrates both the radial expansion from wall deformation *and* a

component of this downstream axial translation. Thus, the derivative of a position-time streak record is not actually a material velocity, but rather the rate of radial increase at an Eulerian location that exceeds the actual cylinder wall velocity as shown in Fig. 4. The analytic form of this value is presented as Equation 3 in Jackson [19].

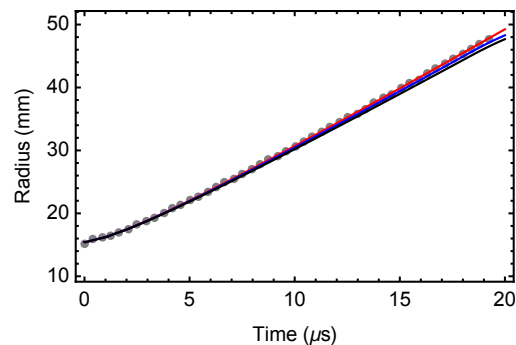


Figure 4: Data from 8-1293. The black curve is the integrated velocity component measured by the probe. The blue curve is the integral of the computed total velocity. The red curve is the computed integral of the rate of radial increase. The gray points are the actual streak record from the same experiment. The agreement of the red curve and gray points validates the probe correction methods of Jackson [19, 24, 25].

Heterodyne doppler interferometer systems, such as PDV, utilize a different measurement principle. A single wavelength of light is emitted from the probe, reflected and Doppler-shifted from the moving target, and then recollects by the probe. The returned Doppler-shifted light is combined with light of the incident wavelength. The resulting small difference in wavelengths interferes to form a measurable beat frequency, which analytically translates to a particle velocity. Light is only Doppler-shifted by the component of wall particle velocity in the direction of the probe. As a result, if the total wall velocity vector is not directly aligned with the probe measurement axis, only a component of the total wall velocity will be measured (corresponding to the product of the wall velocity and the cosine of the angle between total velocity vector and the probe axis). Additionally, no translation movement (such as sliding or transverse motion) normal to the probe is measured as it does not Doppler-shift the light [26]. Thus, generally, a PDV record only reports a component of the total wall velocity that varies with time as the cylinder angle increases. The instantaneous wall angle and total velocity can be recovered from a normally oriented PDV probe [19, 25] or angled probe [24].

Figure 4 demonstrates the difference between these velocity components using data from test 8-1293. The integrated radial increase rate (gray) from the streak

record is 2% larger than the integrated total velocity (blue) computed from the raw probe data (black) via Jackson [19]. The integral of the directly measured PDV velocity (black) is approximately 2% lower than the integral of the total velocity record. Thus, uncorrected streak “velocities” from McMurphy [21] and Campbell and Engelke [22] overestimate the total cylinder wall velocity by approximately 2%. Transforming the measured PDV velocity component (black) to the corresponding radial increase rate using the method of Jackson [24] yields the red curve, which agrees excellently with the experimental streak record (gray). This serves as validation of the theories presented in Jackson [19, 24, 25].

### 3.2. Energy Delivery to Confiner with Age

We evaluate the performance degradation of aged PBX 9404 using the energy imparted to the copper confiner tube in the CYLEX geometry. This is the most direct approach that can be applied to the available data to analyze the effect of HE age on energy delivery while accounting for variations in the initial cylinder wall thickness.

All data from Table 1 was corrected to yield the total cylinder kinetic energy as a function of radius. For the streak data, this involved fitting Eq. 4 in Jackson [20] to the radius-time streak camera record. Fit parameters for that equation of wall motion are given in Table 3. The equation was then differentiated with respect to time to yield the radial rate of increase with time for each streak record. This data was then used as input to Eq. 3 in Jackson [19] to yield the full kinematic history of the cylinder.

Table 3: Parameter estimates for Eq. 4 in Jackson [20] fit to wall motion records for the tests detailed in Table 1.

Identifier	$v_\infty$ (mm/ $\mu$ s)	$a_0$ (mm/ $\mu$ s)	$\omega$
K260235 $\blacktriangle$	2.300	2.220	0.37
K260237 $\blacktriangle$	2.096	2.147	0.51
K260273 $\blacktriangle$	1.923	1.488	0.83
C4526 $\bullet$	2.013	1.588	0.74
C4527 $\bullet$	2.000	1.510	0.78
8-1292 $\bullet$	1.866	1.062	1.00
8-1293 (streak) $\bullet$	1.943	1.517	0.78
8-1293 (PDV) $\bullet$	1.867	1.088	1.00
8-1874 $\bullet$	1.937	1.608	0.75
8-1875 $\bullet$	2.027	1.950	0.56

Data from the PDV diagnostic was analyzed in similar fashion, the only difference being that the PDV data from the probes that were oriented normally to the initial position of the cylinder wall serves as input to Eq. 1 in Jackson [19]. For the PDV data of test 8-1293, where

the probe was oriented 7° off normal to the initial position of the cylinder wall, the measured cylinder velocity was corrected to generate the normal velocity using the angle correction method [24] and then processed as noted above.

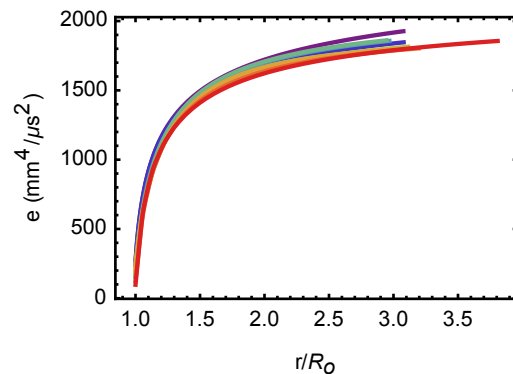


Figure 5: Density-normalized kinetic energy of the cylinder wall versus nondimensional radius with colors as indicated in Table 3.

Figure 5 plots the results of the above analysis in the form of the total cylinder energy (normalized by the explosive initial density) versus the normalized outer wall radius. The density-normalized total cylinder energy is  $e = \rho_c V^2 A / \rho_0$ , where  $\rho_c$  is the copper density,  $\rho_0$  is the initial explosive density,  $V$  is the total cylinder wall velocity, and  $A$  is the cross sectional area of the cylinder, which is assumed to be constant with time such that  $A = \pi(r^2 - r_i^2) = \pi(R_o^2 - R_i^2)$  with  $r$  and  $r_i$  as instantaneous outer and inner radii and with  $R_o$  and  $R_i$  as initial outer and inner radii. The color of each curve indicates the age of explosive using an RGB scale as shown in Table 1, with bluer colors indicating younger explosive at the time of the cylinder test (corresponding to older test data). The data trend indicates that older explosive delivers less energy to the copper wall for all radii.

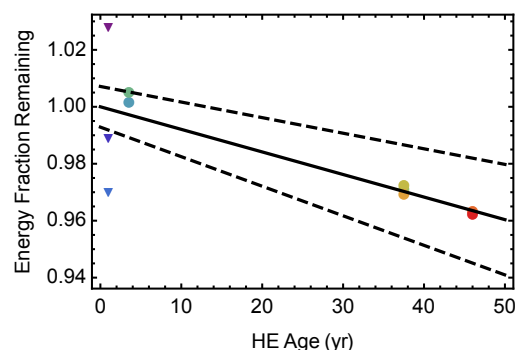


Figure 6: Relative energy versus age at  $r/R_o = 3.0$  with symbols as indicated in Table 3. The solid black line is the fit and the dashed lines indicate the uncertainty bounded by the parameter standard error estimates.

Figure 6 plots the calculated wall energy at a fixed

radius of  $r/R_o = 3.0$ , corresponding to an approximate product specific volume of 7.0 cc/g, which is at the start of the incompressible cylinder motion regime. A linear trend  $e = B(r) - M(r)Y$ , with  $Y$  indicating explosive (or HE) age in years, has been fit to the data to capture the decrease in wall energy with explosive age. The vertical axis has been normalized by the vertical (e-)intercept of the fitted trend to show the fraction of energy remaining in the aged explosive relative to the extrapolated initial energy value. The linear aging trend indicates that the PBX 9404 loses 0.8% of its energy content per decade of age, a value that is consistent prior analysis [12]. The sparse data yields a good fit to the linear trend, though additional data at intermediate ages of 5–35 years would obviously be desirable. The LLNL data also exhibits a large amount of variability relative to the LANL data, but is centered on the trend.

Applying this analysis for all radii allows study of the variation in the linear parameter estimates ( $M$  and  $B$ ) with wall radius. Below, we evaluate the linear trend parameters when fit to all the cylinder data in Table 1 (black curves) and when fit only to the higher resolution LANL data (blue curves).

The evolution of parameter  $B$  with radius is shown in Fig. 7 (top) as the solid line. The dashed lines indicate the possible variation in  $B$  as computed from the standard error associated with the fit at each radius. The trend indicates increasing energy delivered to the wall with increasing radius (or product volume), consistent with the cylinder test method, and the standard error bands indicate high confidence in the calculated fit. Only the fit to the full dataset is shown as there is very little variation in the quantitative trend when fit to only the LANL data.

Figure 7 (bottom) shows the evolution of parameter  $M$  with radius. The behavior is more complex and varies with the input data. Fitting to the LANL data only yields a trend where  $M$  monotonically increases with radius, approaching an apparent asymptote at large expansion values. The standard error bands are small for  $r/R_o$  below 3, but increase substantially for larger radii, indicating variability in late stage expansion behavior across different cylinder tests. This variation is expected as failure of the wall typically onsets in this region [25], limiting the test utility at larger radii. In contrast, fitting to all CYLEX data yields a trend where  $M$  exhibits a local maximum at  $r/R_o = 1.1$ , a local minimum at  $r/R_o = 1.7$  and then monotonically increases for all larger  $r/R_o$ . The standard error bands are significantly larger across all  $r/R_o$  values, consistent with the large variability in the LLNL data. Thus, while there is variation in the behavior of  $M$  with varying input data,

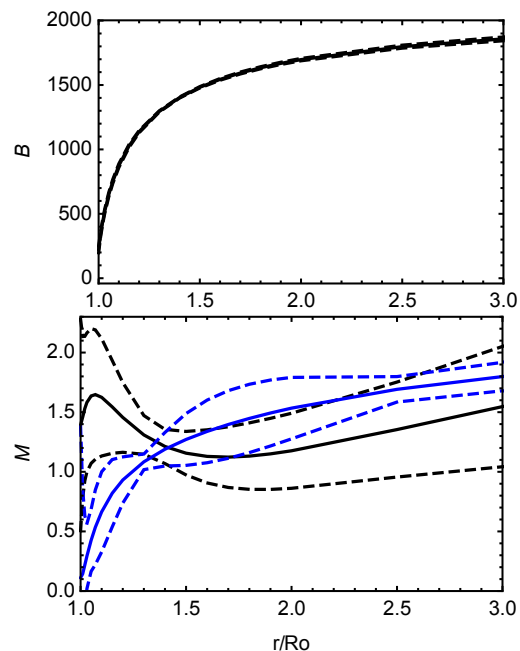


Figure 7: Variation of linear fit term  $B$  (top) and  $M$  (bottom).

both approaches indicate that the observed trend of performance degradation with age is significant for  $r/R_o$  from 1–3.

#### 4. Conclusions

Variations in the explosive performance of naturally aged PBX 9404 were evaluated using the detonation cylinder expansion test. Two cylinder tests were fielded with the oldest known existing PBX 9404 explosive (>46 years). This data was compared with prior PBX 9404 cylinder test data fielded when the explosive was 3–38 years old. A method was also presented to correct for wall motion data collected across differing streak camera and laser interferometry based diagnostics.

This analysis indicated that the aged explosive exhibits decreased performance as inferred from lower energies delivered to the cylinder wall. The degree of this energy decrement varied with cylinder expansion radius (and thus product specific volume). The energy decrement was found to be approximately 0.8% of the total initial explosive energy per decade of age when the products had expanded to 7.0 cc/g. The variation in the trend of  $M$  with radius implies that that the net effect of the observed performance degradation with age will depend on how far the product volume is expanded in each test geometry, with geometries using larger product volumes experiencing increased energy deficits.

Tests with explosive aged for at least 37 years measured energy loss exceeding the chemical energy content of the nitrocellulose binder present in the PBX 9404, implying that the decomposing nitrocellulose also degrades the normally stable HMX ingredient. Such a result is significant as HMX and nitrocellulose are commonly used energetic materials in the propellant and defense industries. These findings indicate that substantial degradation of the energetic material is possible with age and that explosive aging studies should take into account the possibility of reactive decomposition radicals from unstable ingredients degrading normally stable ingredients.

## References

- [1] S. I. Jackson, *Combustion and Flame* 190 (2018) 240–251.
- [2] H. Leider, D. Seaton, Gas evolution and weight loss from thermal decomposition of PBX-9404 below 100 C, Technical Report UCRL-52692, LLNL, 1979.
- [3] G. Perrault, M. Bédard, R. Lavertu, M. Tremblay, *Propellants, Explosives, Pyrotechnics* 4 (1979) 45–49.
- [4] H. Golopol, N. Hetherington, K. North, *Journal of Hazardous Materials* 4 (1980) 45–55.
- [5] M. Makhov, A. Zhigach, I. Leipunskii, *Russian Journal of Physical Chemistry B* 9 (2015) 275–282.
- [6] R. W. Phillips, C. A. Orlick, R. Steinberger, *The Journal of Physical Chemistry* 59 (1955) 1034–1039.
- [7] C. MacDougall, D. Remling, H. Kuepper, Detailed examination of aging processes of PBX 9404, Technical Report MHSMP-75-36B, Mason and Hanger-Silas Mason Co., Inc., Amarillo, USA, 1975.
- [8] H. N. Volltrauer, A. Fontijn, *Comb. and Flame* 41 (1981) 313–324.
- [9] S. Chidester, C. Tarver, A. DePiero, R. Garza, *AIP Conference Proceedings* 505 (2000) 663–666.
- [10] C. M. Tarver, T. D. Tran, *Comb. and Flame* 137 (2004) 50–62.
- [11] A. Burnham, L. Fried, Kinetics of PBX 9404 aging, Technical Report UCRL-CONF-224391, LLNL, 2006. 27th Aging, Compatibility and Stockpile Stewardship Conference.
- [12] L. G. Hill, R. Mier, M. E. Briggs, in: *AIP Conference Proceedings*, volume 1195, AIP, pp. 129–132.
- [13] T. Gibbs, A. Popolato, in: *LASL Explosive Property Data*, University of California Press, 1980, pp. 234–249.
- [14] H. Leider, A. Pane, Degradation of the Molecular Weight and Nitrate Ester Content of Cellulose Nitrate on Thermal Aging, Technical Report UCRL-53163, LLNL, 1981.
- [15] X. Shi, J. Wang, X. Li, C. An, *Journal of Propulsion and Power* 31 (2015) 757–761.
- [16] J. Kury, H. Hornig, E. Lee, J. McDonnell, D. Ornellas, M. Finger, F. Strange, M. Wilkins, in: *Proc. 4th Intl. Det. Symp.*, Naval Ordnance Laboratory, ACR-126, pp. 3–13.
- [17] G. Taylor, *Mechanics of Fluids*, Scientific Papers of GI Taylor 2 (1941) 277–286.
- [18] L. Hill, in: *Proceedings of the 21st ISSW*, pp. 1–6. Paper 2780.
- [19] S. Jackson, *Proc. Comb. Inst.* 35 (2015) 1997–2004.
- [20] S. Jackson, in: *Proceedings of the 15th International Detonation Symposium*, Office of Naval Research, 2015, pp. 171–180.
- [21] F. McMurphy, Cylinder Tests of HE Materials, Technical Report UCRL-MI-132777, LLNL, 1988.
- [22] A. Campbell, R. Engelke, Cylinder Test Comparison of PBX 9404, PBX 9501, and X-0282, Technical Report M-3-QR-75-3, pp. 51–54, LANL, 1975.
- [23] L. Hill, R. Mier, M. Briggs, in: *AIP Conference Proceedings*, volume 1195, pp. 129–132.
- [24] S. Jackson, *AIP Conference Proceedings* 1793 (2017) 050017.
- [25] S. Jackson, *Proc. of the Comb. Inst.* 36 (2017) 2791–2798.
- [26] D. Dolan, *AIP Conference Proceedings* 1195 (2009) 589–594.